Article

Programmable heating and quenching for efficient thermochemical synthesis

https://doi.org/10.1038/s41586-022-04568-6

Received: 28 June 2021

Accepted: 20 February 2022

Published online: 18 May 2022

Check for updates

Qi Dong[1,10], Yonggang Yao[1,10], Sichao Cheng[2,10], Konstantinos Alexopoulos[3,8,10], Jinlong Gao[1], Sanjana Srinivas[3], Yifan Wang[3], Yong Pei[4], Chaolun Zheng[4], Alexandra H. Brozena[1], Hao Zhao[5], Xizheng Wang[1], Hilal Ezgi Toraman[3,9], Bao Yang[4], Ioannis G. Kevrekidis[6], Yiguang Ju[5], Dionisios G. Vlachos[3]✉, Dongxia Liu[2]✉ & Liangbing Hu[1,7]✉

Conventional thermochemical syntheses by continuous heating under near-equilibrium conditions face critical challenges in improving the synthesis rate, selectivity, catalyst stability and energy efficiency, owing to the lack of temporal control over the reaction temperature and time, and thus the reaction pathways[1–3]. As an alternative, we present a non-equilibrium, continuous synthesis technique that uses pulsed heating and quenching (for example, 0.02 s on, 1.08 s off) using a programmable electric current to rapidly switch the reaction between high (for example, up to 2,400 K) and low temperatures. The rapid quenching ensures high selectivity and good catalyst stability, as well as lowers the average temperature to reduce the energy cost. Using CH_4 pyrolysis as a model reaction, our programmable heating and quenching technique leads to high selectivity to value-added C_2 products (>75% versus <35% by the conventional non-catalytic method and versus <60% by most conventional methods using optimized catalysts). Our technique can be extended to a range of thermochemical reactions, such as NH_3 synthesis, for which we achieve a stable and high synthesis rate of about 6,000 μmol g_{Fe}^{-1} h^{-1} at ambient pressure for >100 h using a non-optimized catalyst. This study establishes a new model towards highly efficient non-equilibrium thermochemical synthesis.

Thermochemical reactions proceed along specific pathways that are heavily affected by the reaction temperature and time. In particular, the elementary reaction rate is exponentially dependent on temperature according to the Arrhenius law, and the product distribution can be further influenced by establishing or shifting the chemical equilibrium[4,5]. Therefore, dynamic modulation of the heating profile could be used to control the reaction pathways for targeted product yield and selectivity. However, conventional thermochemical reactions are typically conducted by continuous heating under near-equilibrium conditions[4], despite a long history of efforts to develop dynamically heated reactors[1,3,6]. This is in part because conventional heating devices show poor heat transfer and large thermal inertia, which makes it challenging to attain temporal control over the temperature profiles and thus affect the reaction pathways. Taking methane (CH_4) pyrolysis as an example, selective CH_4 transformation to value-added products has proved extremely important but difficult to achieve under continuous heating at a relatively mild temperature regime (<1,400 K)[7]. The constraints of chemical equilibrium often result in limited selectivity, low conversion or both.

Herein, we report a dynamic operating technique that addresses these issues using programmable heating and quenching (PHQ) to conduct thermochemical reactions with a high selectivity, rate and yield to value-added products at low energy cost. Compared with conventional steady-state approaches that operate with continuous heating at constant temperatures (for example, 1,273 K in Fig. 1a), the Joule-heating-based PHQ method allows for rapid switching between low and high temperatures (for example, between 650 and 2,000 K in Fig. 1b) in just milliseconds, simply by varying the electric current applied to a carbon heater to achieve thermochemical synthesis. Such a heating profile is also enabled by placing the porous carbon heater in direct contact with the reactants to establish efficient heat transfer. This design allows the temperature of the gas-phase reactants and the adsorbed surface species on the catalysts to closely follow the temperature profile of the carbon heater, which enables us to precisely control the reaction pathway under non-equilibrium conditions.

Using CH_4 pyrolysis as a model reaction, our PHQ method demonstrates much higher selectivity (>75% versus <35%) to value-added C_2 products at comparable CH_4 conversions (about 13%) in comparison with the conventional catalyst-free CH_4 pyrolysis performed under near-equilibrium conditions by continuous heating[8] (Fig. 1c). The C_2 product selectivity by our metal-catalyst-free PHQ technique even

[1]Department of Materials Science and Engineering, University of Maryland, College Park, MD, USA. [2]Department of Chemical and Biomolecular Engineering, University of Maryland, College Park, MD, USA. [3]Department of Chemical and Biomolecular Engineering, University of Delaware, Newark, DE, USA. [4]Department of Mechanical Engineering, University of Maryland, College Park, MD, USA. [5]Department of Mechanical and Aerospace Engineering, Princeton University, Princeton, NJ, USA. [6]Department of Chemical and Biomolecular Engineering, Department of Applied Mathematics and Statistics, Johns Hopkins University, Baltimore, MD, USA. [7]Center for Materials Innovation, University of Maryland, College Park, MD, USA. [8]Present address: Department of Chemical Engineering, The Pennsylvania State University, University Park, PA, USA. [9]Present address: Department of Energy and Mineral Engineering, The Pennsylvania State University, University Park, PA, USA. [10]These authors contributed equally: Qi Dong, Yonggang Yao, Sichao Cheng, Konstantinos Alexopoulos. ✉e-mail: vlachos@udel.edu; liud@umd.edu; binghu@umd.edu

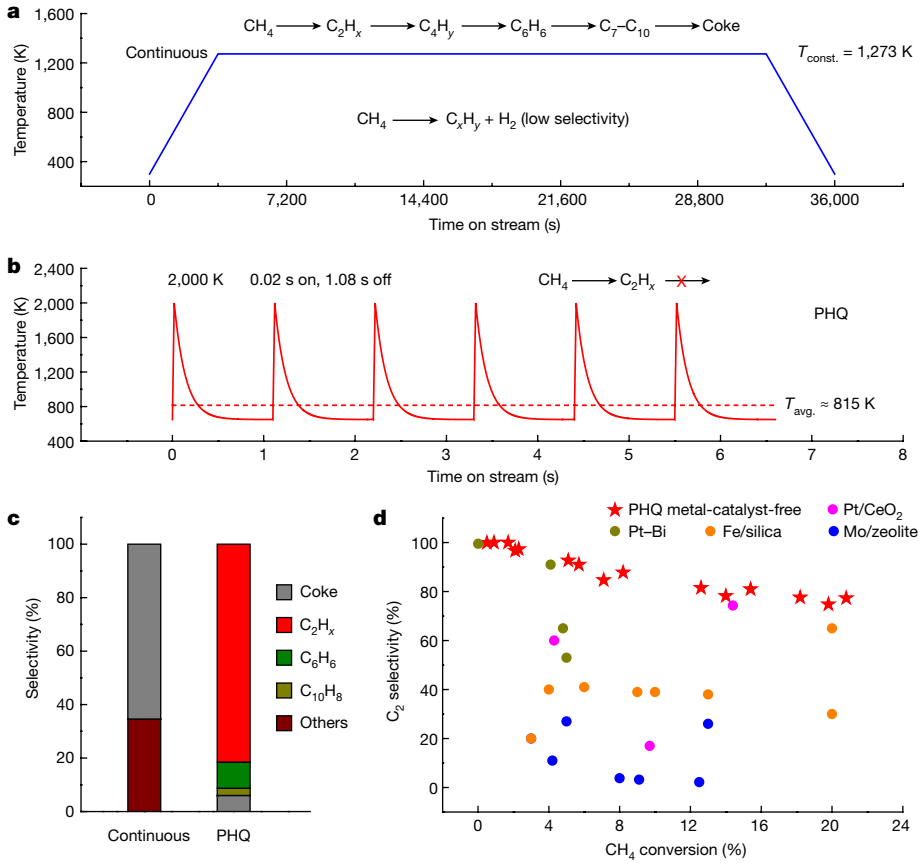

Fig. 1 | Comparison between our PHQ method and conventional continuous heating using a CH_4 pyrolysis model reaction. a, Schematic of a typical temperature profile by continuous heating. Continuous heating creates a variety of products owing to the lack of temporal tunability over the temperature profile and thus the resulting reaction pathways. **b**, Schematic of an estimated temperature profile by the PHQ method. PHQ selectively produces value-added C_2 products. The high temperature ensures high conversion, whereas the transient heating duration enables high selectivity. **c**, Comparison of CH_4 pyrolysis by PHQ in this work and continuous heating reported in the literature[8]. At comparable CH_4 conversions (about 13%), continuous heating of the non-catalytic CH_4 pyrolysis reaction results in coke as the major product (grey) with other minor products (maroon)[8], whereas CH_4 pyrolysis by PHQ showcases its >75% selectivity to C_2 products (red). **d**, Our metal-catalyst-free PHQ technique (red stars) even outperforms most literature reports of CH_4 pyrolysis reactions with optimized catalysts conducted by continuous heating in terms of the C_2 product selectivity at a wide range of CH_4 conversions[9–18].

outperforms most literature reports of CH_4 pyrolysis using optimized catalysts by continuous heating[9–18] (Fig. 1d). The PHQ technique can also be expanded to a variety of thermochemical processes, such as NH_3 synthesis, to achieve high production rates and good stability. This approach establishes a general platform for efficient thermochemical synthesis with a high reaction rate, selectivity, reduced energy cost and improved catalyst stability.

To apply the PHQ technique, we use a sheet of porous carbon paper as the heating element, which is placed along the middle axis of a quartz tube reactor (Fig. 2a and Supplementary Discussion 1). To generate heat, we pass an electric current through the carbon paper, which – owing to its low heat capacity (<0.033 J K^{-1}) – is able to reach ramping and cooling rates of around 10^4 K s^{-1} (ref. [19]) (Fig. 2b and Supplementary Discussion 2). During this process, the gas-phase reactants flow through the reactor and come into direct contact with the carbon paper, passing through and directly interacting with its microstructure (Fig. 2c), thereby closely following its programmed heating pattern. Most of the electrical energy is converted to heat the gas molecules[20], therefore the energy transfer efficiency by PHQ is enhanced compared with conventional processes, in which heaters are generally placed outside the reactor[21,22]. Note that no extra catalyst is needed in the design (Fig. 2c and Supplementary Discussion 3), as the high temperature of the carbon heater exponentially increases the CH_4 activation rate for high conversion. For initial characterization of the PHQ method, we investigated the carbon paper heating element in a 'flat' configuration in the centre of the reactor, which was straightforward to reproduce, although we acknowledge that this setup is not optimized for the spatial uniformity of temperature and CH_4 conversion. However, the structural flexibility of the carbon heater provides the potential to manipulate its shape for enhanced interaction with the gas molecules (Fig. 2d and Supplementary Discussion 4).

In a typical heating programme, we switch the electrical power applied to the carbon heater from the 'off' state to the 'on' state and hold for 0.02 s, followed by removing the power to turn the heater back off for 1.08 s to complete a period of 1.1 s, which is then repeated. By adjusting the input power for a specific pulse duration, the peak temperature (T_{high}) of the carbon heater can also be accurately controlled (Supplementary Discussion 5 and Supplementary Table 1). We demonstrate the ability to tune T_{high} and the pulse duration according to the programmed electrical signal, as shown in Fig. 2e, f, respectively. Using numerical simulations with different peak temperatures, we verify that the temperature profile of the gas molecules that interact with or are near the surface of the carbon paper precisely coincides with that of the heater (Fig. 2g), demonstrating rapid heating and cooling rates (Supplementary Discussion 6 and Supplementary Tables 2 and 3). These results confirm that our PHQ method enables an accurate, temporal temperature pattern experienced by the gas molecules flowing through the reactor and interacting with the carbon heater.

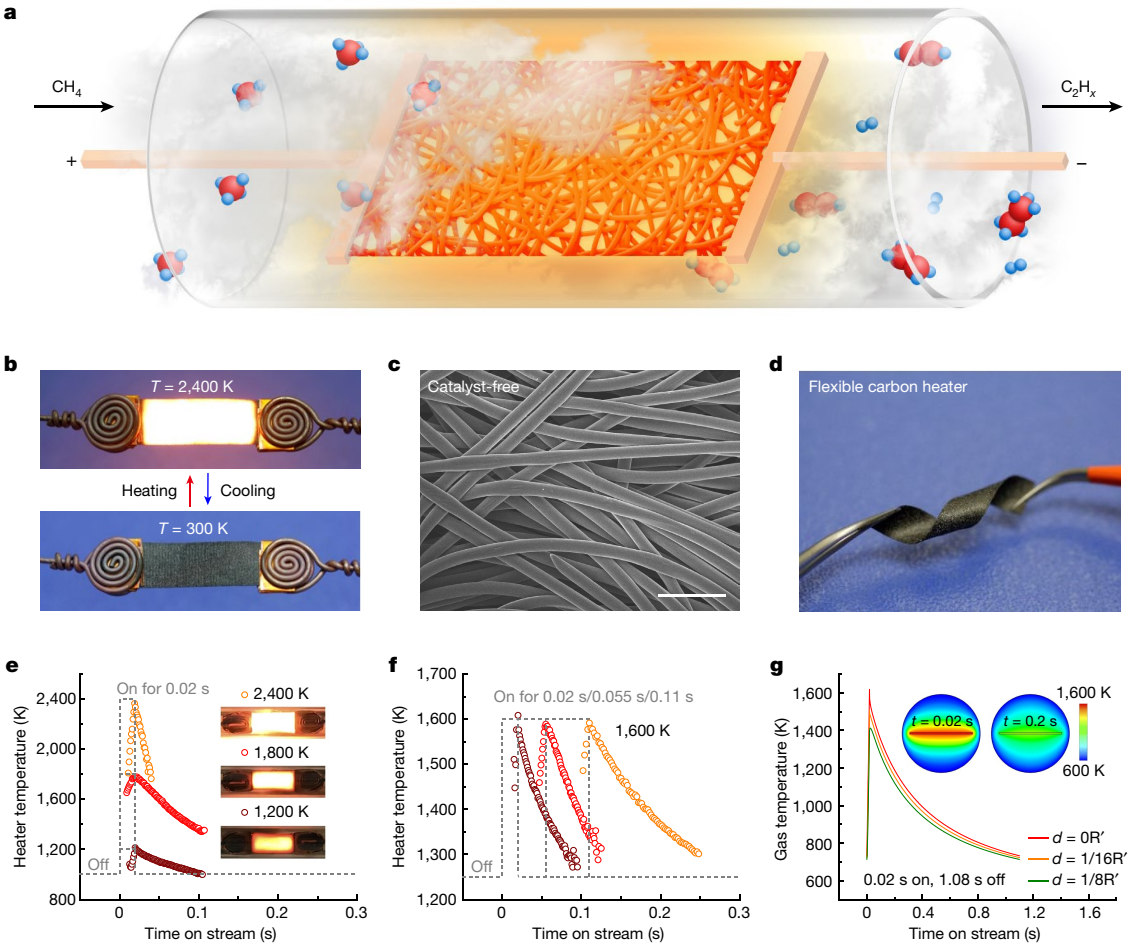

Fig. 2 | Operation of the PHQ technique. a, Schematic of the reactor design. The CH_4 molecules pass through the reactor and interact with the heated porous carbon paper to rapidly transform into desirable value-added C_2 products. **b**, Digital images of the carbon heater in power off (bottom) and power on (top) states, corresponding to the switch from room temperature (about 300 K) to high temperature (about 2,400 K). **c**, Scanning electron microscopy image of the carbon heater, showcasing the highly porous microstructure and the catalyst-free surface. Scale bar, 50 µm. **d**, Digital image of the flexible carbon heater. **e**, The temporal temperature pattern of the carbon heater is tuned by increasing the input electrical power for higher peak temperatures at fixed pulse duration (dashed grey line). Insets are digital images showing the carbon paper being heated to different temperatures. **f**, The temporal temperature profile of the carbon heater can also be tuned by varying the pulse duration at a fixed peak temperature. Increased pulse duration requires decreased power input to reach the same peak temperature. **g**, Numerical simulation verifies that the temporal temperature pattern of the gas molecules closely follows that of the carbon heater (0.02 s on, 1.08 s off; T_{high} = 1,600 K). The three traces represent the temporal temperature patterns of three spatial positions (in the reactor cross-section) vertically above the middle point on the upper surface of the carbon paper with distances (d) of $0R'$, $1/16R'$ and $1/8R'$. R' is the closest distance from the middle point on the upper surface of the carbon heater to the edge of the cylindrical quartz tube reactor ($R' = R - 1/2D$, in which R is the radius of the reactor and D is the thickness of the carbon paper). The insets show the cross-sectional contour maps of the gas temperature distribution when the time on stream equals 0.02 s (when T_{high} is reached) and 0.2 s (when most gas molecules are cooled down).

Figure 3 demonstrates the utility and advantages of our PHQ technique using CH_4 pyrolysis as a model reaction. We compared four different reaction conditions (Fig. 3a), including: (1) non-catalytic CH_4 pyrolysis using continuous furnace heating at 1,273 K; (2) catalytic CH_4 pyrolysis with a state-of-the-art Fe/silica catalyst[7,9,10] using continuous furnace heating at 1,273 K; (3) CH_4 pyrolysis with the carbon paper heating element (as shown in Fig. 2 but without PHQ) using continuous furnace heating at 1,273 K; and (4) CH_4 pyrolysis using our PHQ technique with a T_{high} of 2,200 K and pulse duration of 0.055 s over a period of 1.1 s (0.055 s on, 1.045 s off). We found that the product distribution of our PHQ method showed a notable improvement compared with the other techniques, with a much higher selectivity (around 80%) for C_2 products. In comparison, only about 40% C_2 products were measured using continuous heating by a furnace at 1,273 K with the Fe/silica catalyst, which is consistent with the literature[9]. For the non-catalytic system, continuous furnace heating at 1,273 K produced nearly zero product. Meanwhile, continuous heating in the presence of the carbon paper (using a furnace, without PHQ) showed a large amount of undesired coke (about 30%) and low C_2 product selectivity (about 40%)[23,24] (Fig. 3a). These results indicate that low C_2 selectivity is intrinsic to the continuous heating method owing to marked secondary and subsequent reactions, resulting in the formation of low-value compounds, such as naphthalene and coke. By contrast, PHQ can achieve stable and high selectivity to C_2 products with limited coke formation (Supplementary Discussion 7). Notably, with an average temperature ($T_{avg.}$) of <900 K, PHQ can obtain a comparable CH_4 conversion (about 15%) and much higher value-added C_2 product selectivity than those by the Fe/silica catalyst using continuous heating at 1,273 K (refs. [9,10]) (Fig. 3a).

We further explored the effect of T_{high} and the pulse duration on the CH_4 pyrolysis reaction by programming the electrical signal (Supplementary Discussion 8). In this experiment, we used a lower flow rate (4 sccm, 75 mol% CH_4 and 25 mol% Ar) to increase the CH_4 conversion to

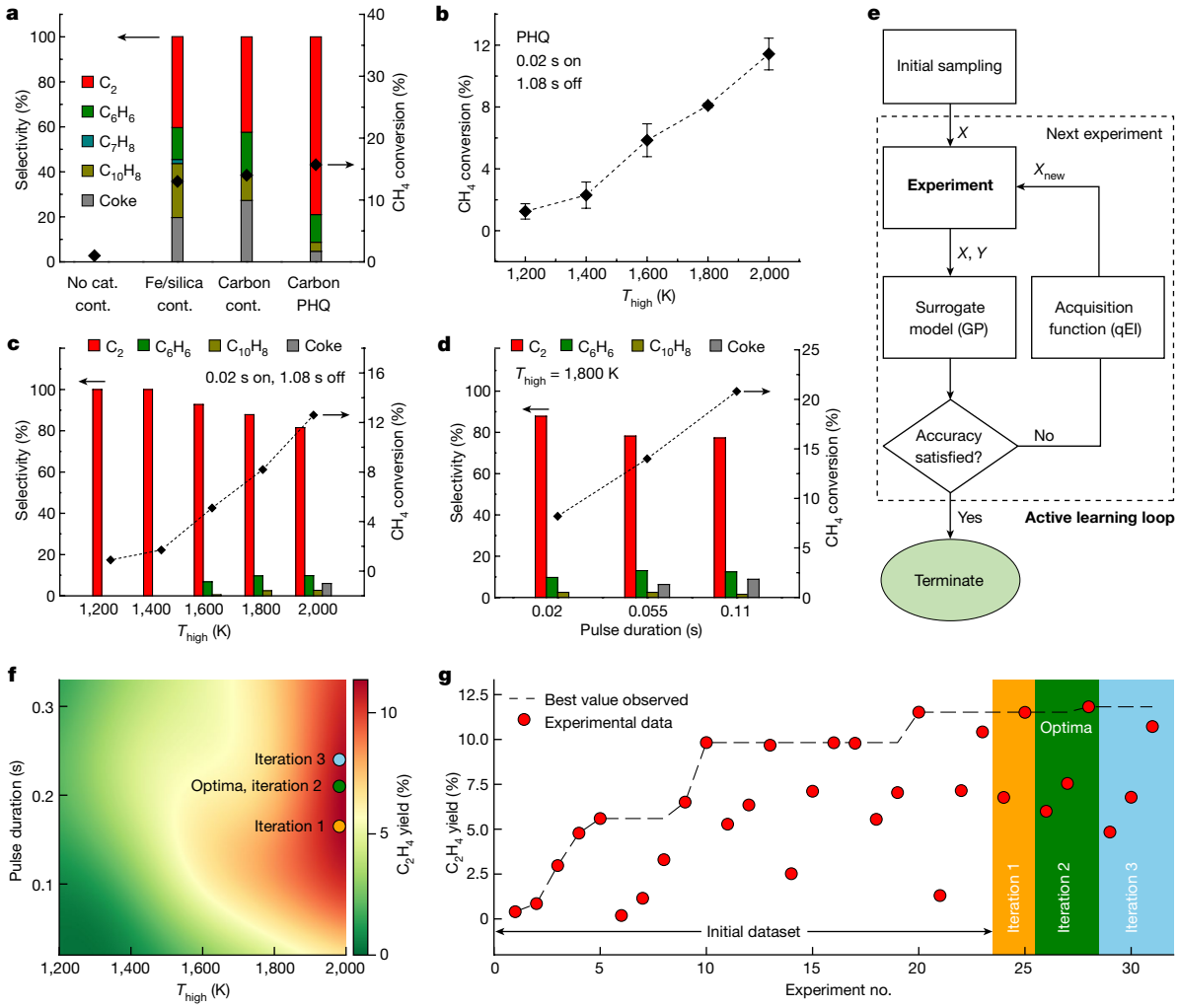

Fig. 3 | The utility and advantages of our PHQ technique. a, Comparison between (from left to right): (1) non-catalytic CH_4 pyrolysis using continuous furnace heating at 1,273 K; (2) catalytic CH_4 pyrolysis with a state-of-the-art Fe/silica catalyst using continuous furnace heating at 1,273 K; (3) CH_4 pyrolysis with carbon paper using continuous furnace heating at 1,273 K; (4) CH_4 pyrolysis using PHQ with a T_{high} of 2,200 K and pulse duration of 0.055 s over a period of 1.1 s (0.055 s on, 1.045 s off, $T_{avg.}$ < 900 K). A flow rate of 24 sccm was used for all four reaction conditions. **b**, CH_4 conversion increases with T_{high} monotonically by PHQ, as demonstrated using a pulse duration of 0.02 s over a period of 1.1 s (0.02 s on, 1.08 s off). Error bars denote standard deviation with the value of $n \geq 3$. **c**, Product selectivity by PHQ at various T_{high} values with a fixed pulse duration of 0.02 s on and 1.08 s off. **d**, Product selectivity by PHQ using various pulse durations at a fixed T_{high} of 1,800 K. A flow rate of 4 sccm was used for **b**–**d**. The error range for C_2 product selectivity was found to be ±3%. **e**, Bayesian-optimization-based active learning framework to optimize the desired product (C_2H_4) yield. **f**, The surrogate model response surface of the C_2H_4 yield as a function of T_{high} and the pulse duration. The red colour indicates a high C_2H_4 yield. The dots represent the sampled experimental data points on the basis of the prediction by the acquisition function. **g**, The optima and experimental C_2H_4 yield in each active learning iteration, corresponding to the experiment numbers.

better resolve these effects. With a fixed pulse duration of 0.02 s on and 1.08 s off, CH_4 conversion increases with T_{high} monotonically (Fig. 3b). Note that increased T_{high} at fixed pulse duration (0.02 s) leads to slightly lower selectivity to the C_2 products but higher selectivity to benzene (C_6H_6) owing to the increased reaction rate at higher temperatures (Fig. 3c). Meanwhile, increasing the pulse duration at a constant T_{high} (1,800 K) leads to a similar trend owing to the longer reaction progress (Fig. 3d). In general, the observed selectivities of the total C_2 products (for example, >75%) by the metal-catalyst-free PHQ process are among the best reported in the literature at comparable CH_4 conversions[9–18].

Compared with continuous heating, PHQ offers a new dimension of tunability by means of the highly controllable variables of the temporal temperature pattern, which can be used by recently developed data science approaches for efficient process optimization[25], thereby greatly reducing the experimental effort compared with conventional trial-and-error methods. To use this advantage, we used Bayesian-optimization-based active learning[26] (Fig. 3e) to help us determine the optimal C_2H_4 yield (see Supplementary Methods for details). Through three iterations in the active learning loop (Fig. 3f and Supplementary Discussion 9), we found that T_{high} = 2,000 K and pulse duration = 0.21 s were the conditions to achieve the highest C_2H_4 yield (11.82%, iteration 2 in Fig. 3g) in our experiments and notably with a $T_{avg.}$ of <1,000 K. The PHQ process can also be driven by active learning to further optimize the yield of multiple products (Supplementary Discussion 10). In this manner, the model can guide us on how to program the heating pattern to lower the undesired product yield at a given target performance with minimal experimental effort. It can also help us rationalize how the relative scaling between the pulsed heating durations and the characteristic time constants of the dominant kinetic pathways leads to improved performance.

We suggest that the rapid heating and quenching processes of the PHQ synthesis provide a greater degree of control by matching the

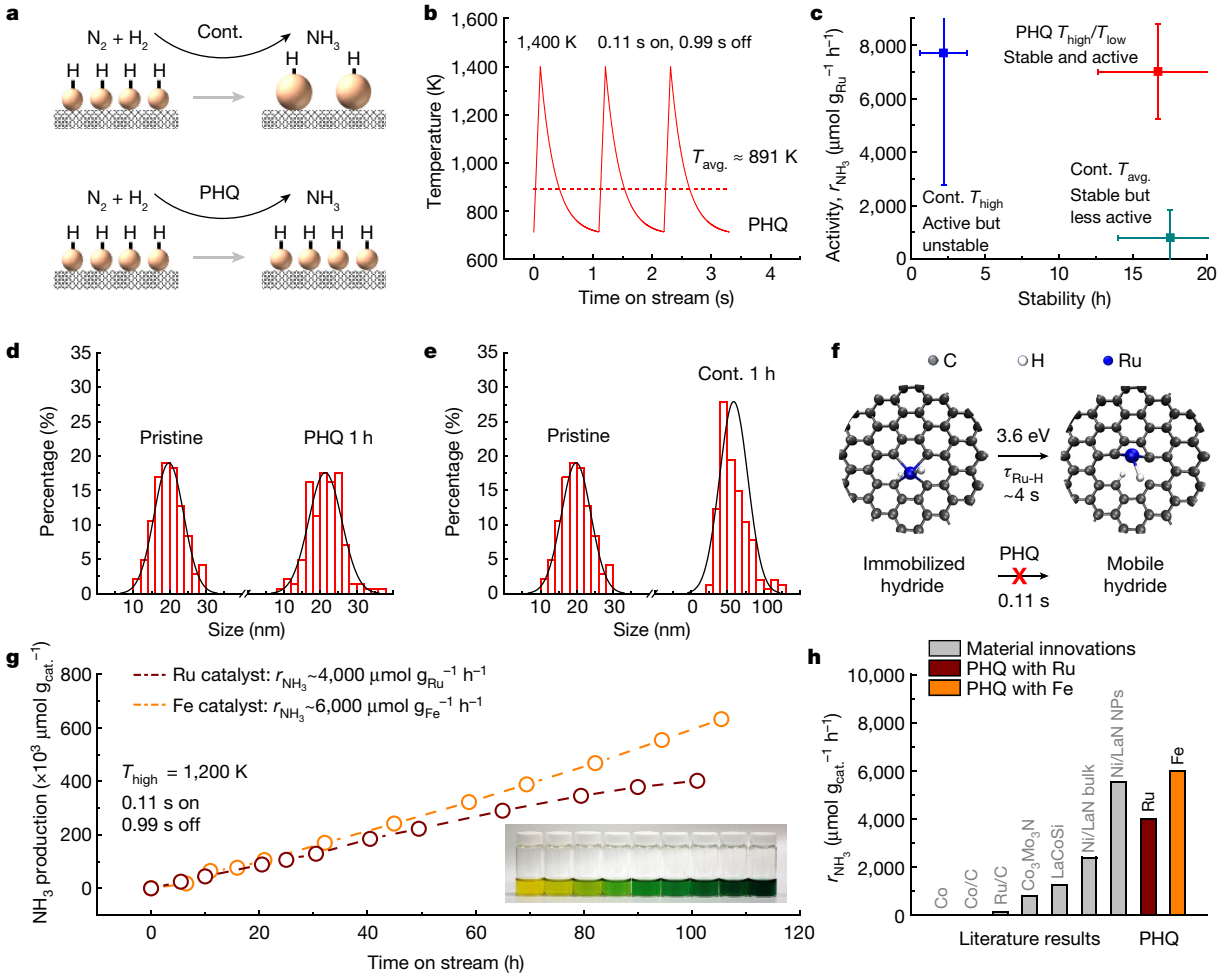

Fig. 4 | NH_3 synthesis by PHQ under ambient pressure. a, Catalyst morphological evolution by means of the metal hydride intermediate during NH_3 synthesis by continuous heating and PHQ. **b**, An estimated temperature profile of the PHQ process used in **c**. **c**, Comparison of the activity and stability of NH_3 synthesis by PHQ (0.11 s on, 0.99 s off; T_{high} of 1,400 K, T_{low} of around 700 K and $T_{avg.}$ of around 900 K) (red) and by continuous heating at 1,400 K (corresponding to T_{high} of PHQ) (blue) and 900 K (corresponding to $T_{avg.}$ of PHQ) (cyan). Error bars denote standard deviation with the value of $n \geq 3$. **d**, Ru catalyst size and distribution after PHQ for 1 h (0.11 s on, 0.99 s off; T_{high} of 1,400 K). **e**, Ru catalyst size and distribution after continuous heating for 1 h at 1,400 K (corresponding to T_{high} of PHQ). **f**, DFT modelling for the activation barrier and timescale of Ru hydride (Ru-H) migration at 1,300 K. **g**, NH_3 production as a function of the time on stream by PHQ (0.11 s on, 0.99 s off; T_{high} of 1,200 K) using non-optimized Ru and Fe catalysts. The error range for production rate was found to be ±3%. The inset shows the testing solutions for NH_3 quantification by the Berthelot method[40]. **h**, Comparison of r_{NH_3} between the PHQ method using non-optimized Ru and Fe catalysts and literature reports on the basis of material innovations[37–39]. NPs, nanoparticles.

formation timescales of the intermediate C_2 species in the CH_4 pyrolysis reaction network but without allowing a steady state to be reached that would lead to secondary and subsequent products[27]. To investigate the mechanism behind the high C_2 product selectivity of our technique, we used first-principles-based microkinetic simulations to compare the continuous heating and PHQ methods. We modelled two types of reactor operated at steady state (that is, under an isothermal condition) and transient modes (that is, using a rapid temperature ramp followed by an exponential decay) to simulate continuous heating and PHQ, respectively (Supplementary Discussion 11). In the steady-state continuous-heating mode, the simulated selectivity to C_6H_6 species is notably high, indicating a large amount of secondary and subsequent reaction products. Compared with continuous heating, PHQ offers higher selectivity to C_2H_6 and C_2H_4 and lower selectivity to C_2H_2 and C_6H_6 (Supplementary Discussion 12). These results are in good agreement with our experimental observations in terms of the high C_2 product selectivity. Beyond the enhanced C_2 product selectivity, our calculations also show that PHQ potentially reduces the average energy needed by >80% compared with continuous heating at identical CH_4 conversion. This feature can be generalized for other reaction schemes, in which PHQ with pulse durations of less than 0.33 s could greatly reduce the energy cost compared with continuous heating (Supplementary Discussion 13).

To understand the role of pulse duration by PHQ, we simulated the characteristic trajectories of CH_4 conversion and product yields up to C_6H_6 as a function of the astronomic time (that is, clock time or external time of the system)[5,28] under isothermal conditions (T = 1,500 K) (Supplementary Discussion 12). The transition from the transient regime (that is, in which the conversion and selectivity change over time before reaching equilibrium) to the steady-state regime requires >0.25 s. Note that the reaction pathway proceeds as $CH_4 \rightarrow C_2H_6 \rightarrow C_2H_4 \rightarrow C_2H_2 \rightarrow C_6H_6$ (refs. [29,30]), in which C_6H_6 forms later than C_2 species after an induction period (that is, a later onset time) owing to the slow bimolecular nature of the cyclization reaction. Hence, transient pulse durations by PHQ (for example, 0.02 s and 0.055 s) can provide enough thermal energy to drive the CH_4 pyrolysis reaction to C_2 species but quench it before a large fraction of C_6H_6 is produced as the reaction approaches steady state. A detailed reaction pathway analysis from CH_4 to C_6H_6 shows that the PHQ method reduces the formation of propargyl radicals (C_3H_3•) by keeping the

pulse durations shorter than the timescale for the cyclization reaction[29,30] (Supplementary Discussion 12). Under transient thermal excitation (PHQ), most of the reaction flux is distributed in reactions among C_2 species and the cyclization reaction from C_3H_3• is limited. By contrast, under steady state (continuous heating), the reaction flux is more uniformly distributed among all the simulated elementary steps of CH_4 pyrolysis, allowing the recombination of C_3H_3• to form aromatic species (Supplementary Discussion 12).

Our PHQ process can also be applied to other thermochemical reactions beyond CH_4 pyrolysis, which is homogeneous and endothermic. To demonstrate its broad applicability, we selected ammonia (NH_3) synthesis (from N_2 and H_2) as a model system that is heterogeneous and exothermic. NH_3 synthesis often suffers from problems such as poor catalyst stability and a low reaction rate by conventional methods[31]. For example, the prevalent metal hydride intermediate species in the presence of H_2 is critical for the NH_3 formation but has a profound impact on the catalyst stability[32,33]. In addition, although high temperature is favourable for N_2 activation, it undermines the catalyst stability by accelerating its sintering process during continuous heating. To resolve these conflicts, we use the PHQ process to enable transient high-temperature heating and therefore a high NH_3 production rate while ensuring good catalyst stability by rapidly quenching the reaction temperature (Fig. 4a). Ru nanoparticles (supported on a carbon felt heater) was selected as a model catalyst, as it shows activity for N_2 activation[31].

Using a typical heating and quenching programme (0.11 s on, 0.99 s off; T_{high} of 1,400 K; an estimated temperature pattern is shown in Fig. 4b), the PHQ operation showed a stable performance that lasted for around 20 h with an NH_3 synthesis rate of about 7,000 μmol g_{Ru}^{-1} h^{-1}, after which the activity started to decay (Fig. 4c). In comparison, we measured the NH_3 synthesis rates by continuous heating at T_{high} (1,400 K), T_{low} (about 700 K) and $T_{avg.}$ (about 900 K). Among these testing conditions (Fig. 4c), continuous heating at T_{high} showed good activity that was comparable with PHQ but only lasted for about 2 h. Meanwhile, continuous heating at $T_{avg.}$ showed much worse catalyst activity, albeit with a stable NH_3 synthesis rate. Last, continuous heating at T_{low} showed an almost zero NH_3 synthesis rate owing to the poor N_2 activation under low temperature (not shown in the figure). We found that the Ru nanoparticles retained their original size and distribution after PHQ for 1 h (Fig. 4d) but severely sintered after continuous heating at T_{high} for the same duration (Fig. 4e and Supplementary Discussion 14). Taking the morphological evolution of the catalyst into consideration, we simulated the scenarios of NH_3 synthesis by PHQ and continuous heating at a series of temperatures[34]. The results agree well with our experimental observation that PHQ offers highly stable and fast NH_3 production rates (Supplementary Discussion 14).

We used density functional theory (DFT) calculations to understand how PHQ improves the catalyst stability. Ru hydride (Ru-H) species should be readily available under NH_3 synthesis conditions, as the adsorption/dissociation of H_2 is common on metal catalyst surfaces[32]. Our DFT calculations estimated the potentially rate-determining step for the diffusion of Ru-H on the carbon support to have an activation energy of about 3.6 eV and a corresponding timescale of approximately 4 s ($\tau_{Ru\text{-}H}$, Fig. 4f). Furthermore, defects on the carbon support are critical for anchoring catalysts[35] but self-heal at high temperatures[36]. We estimated the corresponding activation energy and timescale of this process to be about 3.7 eV and about 8 s, respectively (Supplementary Discussion 15). The timescales (4–8 s) of these two processes are an order of magnitude longer than the pulse duration of PHQ (0.11 s). As a result, the PHQ method is able to quench these detrimental processes before they can lead to the migration of Ru atoms on the carbon support. In comparison, continuous heating does not offer this amount of control against catalyst sintering.

Owing to the improved catalyst stability, we were able to maintain stable NH_3 production for 100 h with an average synthesis rate r_{NH_3} of about 4,000 μmol g_{Ru}^{-1} h^{-1} by PHQ (0.11 s on, 0.99 s off; T_{high} of 1,200 K) using a non-optimized Ru catalyst (Fig. 4g). We also demonstrated stable NH_3 production for >100 h using a non-optimized Fe catalyst ($\tau_{pulse} < \tau_{Fe\text{-}H}$, Supplementary Discussion 15) with an average synthesis rate r_{NH_3} of around 6,000 μmol g_{Fe}^{-1} h^{-1} (Fig. 4g), which is among the highest in the literature under ambient pressure[37–39] (Fig. 4h). Furthermore, compared with literature-reported continuous heating using a similar Ru/C catalyst[39], the r_{NH_3} of the PHQ process is more than an order of magnitude higher. We attribute this performance to the high temperature that is enabled by PHQ without sacrificing the catalyst stability because of the rapid temperature quenching. Recently, Hosono and colleagues reported a Ni-loaded LaN catalyst for stable NH_3 synthesis at a high r_{NH_3} under ambient pressure[37]. Unlike this breakthrough in material development, PHQ offers a new and general process that boosts the activity and stability of non-optimized catalysts (for example, Ru and Fe) to a comparably high performance level[37] (Fig. 4h). We predict that our PHQ process can be potentially coupled with such material innovations for even greater thermochemical synthesis outcomes.

In this study, we demonstrate the PHQ thermochemical synthesis technique using the CH_4 pyrolysis reaction as a proof of concept. The process, without using metal-based catalysts, enables a high selectivity to value-added C_2 products. Our study opens up a new model for implementing a range of industrially important thermochemical processes, such as NH_3 synthesis. We show that PHQ prevents catalyst sintering, thereby achieving a stable and high NH_3 synthesis rate under ambient pressure. In general, the high temperature in the PHQ technique enables fast activation of reactants for high rates and conversions, and the precise control over the heating process leads to high selectivities of desired products and improved catalyst stability. Although the quenching process is not actively controlled, tuning the electric current can potentially create complex and sculpted temperature patterns (for example, square wave, triangle wave, stepped heating and cooling, and so on) to accurately manipulate the reaction pathways.

Scaling up the PHQ reactor relies on increasing the size of the carbon heater, which needs to be porous to allow gas molecules to diffuse throughout the structure, and – at the same time – possess a low total heat capacity for rapid heating and cooling. Commercial materials such as carbon felt and carbon foam can be used. Specially designed and synthesized carbon materials are also promising candidates. For example, the carbon heater can be highly porous three-dimensional structures and assembled to arrays for large-scale operations. Driven by electrical energy, our technique may also enable process intensification and distributed chemical manufacturing with improved efficiency[21,22].

Online content

Any methods, additional references, Nature Research reporting summaries, source data, extended data, supplementary information, acknowledgements, peer review information; details of author contributions and competing interests; and statements of data and code availability are available at https://doi.org/10.1038/s41586-022-04568-6.

1. Bailey, J. E. Periodic operation of chemical reactors: a review. *Chem. Eng. Commun.* **1**, 111–124 (1973).
2. Wolff, J., Papathanasiou, A. G., Kevrekidis, I. G., Rotermund, H. H. & Ertl, G. Spatiotemporal addressing of surface activity. *Science* **294**, 134–137 (2001).
3. Kevrekidis, I. G., Schmidt, L. D. & Aris, R. Some common features of periodically forced reacting systems. *Chem. Eng. Sci.* **41**, 1263–1276 (1986).
4. Chorkendorff, I. & Niemantsverdriet, J. W. *Concepts of Modern Catalysis and Kinetics* 3rd edn (Wiley, 2017).
5. Marin, G. B., Yablonsky, G. S. & Constales, D. *Kinetics of Chemical Reactions: Decoding Complexity* 2nd edn (Wiley, 2019).
6. Papathanasiou, A. G., Wolff, J., Kevrekidis, I. G., Rotermund, H. H. & Ertl, G. Some twists and turns in the path of improving surface activity. *Chem. Phys. Lett.* **358**, 407–412 (2002).
7. Guo, X. et al. Direct, nonoxidative conversion of methane to ethylene, aromatics, and hydrogen. *Science* **344**, 616–619 (2014).
8. Calkins, W. H. & Bonifaz, C. Coal flash pyrolysis: 5. Pyrolysis in an atmosphere of methane. *Fuel* **63**, 1716–1719 (1984).

9. Hao, J. et al. Enhanced methane conversion to olefins and aromatics by H-donor molecules under nonoxidative condition. *ACS Catal.* **9**, 9045–9050 (2019).
10. Sakbodin, M., Wu, Y., Oh, S. C., Wachsman, E. D. & Liu, D. Hydrogen-permeable tubular membrane reactor: promoting conversion and product selectivity for non-oxidative activation of methane over an Fe@SiO_2 catalyst. *Angew. Chem. Int. Ed.* **55**, 16149–16152 (2016).
11. Šot, P. et al. Non-oxidative methane coupling over silica versus silica-supported iron(II) single sites. *Chem. Eur. J.* **26**, 8012–8016 (2020).
12. Wu, Y. et al. Overgrowth of lamellar silicalite-1 on MFI and BEA zeolites and its consequences on non-oxidative methane aromatization reaction. *Microporous Mesoporous Mater.* **263**, 1–10 (2018).
13. Liu, L. et al. Methane dehydroaromatization on Mo/HMCM-22 catalysts: Effect of SiO_2/Al_2O_3 ratio of HMCM-22 zeolite supports. *Catal. Lett.* **108**, 25–30 (2006).
14. Zhang, Y. et al. Promotional effects of In on non-oxidative methane transformation over Mo-ZSM-5. *Catal. Lett.* **146**, 1903–1909 (2016).
15. Aboul-Gheit, A. K., Awadallah, A. E., Aboul-Enein, A. A. & Mahmoud, A.-L. H. Molybdenum substitution by copper or zinc in H-ZSM-5 zeolite for catalyzing the direct conversion of natural gas to petrochemicals under non-oxidative conditions. *Fuel* **90**, 3040–3046 (2011).
16. Bajec, D., Kostyniuk, A., Pohar, A. & Likozar, B. Micro-kinetics of non-oxidative methane coupling to ethylene over Pt/CeO_2 catalyst. *Chem. Eng. J.* **396**, 125182 (2020).
17. Xie, P. et al. Nanoceria-supported single-atom platinum catalysts for direct methane conversion. *ACS Catal.* **8**, 4044–4048 (2018).
18. Xiao, Y. & Varma, A. Highly selective nonoxidative coupling of methane over Pt-Bi bimetallic catalysts. *ACS Catal.* **8**, 2735–2740 (2018).
19. Butland, A. T. D. & Maddison, R. J. The specific heat of graphite: an evaluation of measurements. *J. Nucl. Mater.* **49**, 45–56 (1973).
20. Bao, W. et al. Flexible, high temperature, planar lighting with large scale printable nanocarbon paper. *Adv. Mater.* **28**, 4684–4691 (2016).
21. Van Geem, K. M., Galvita, V. V. & Marin, G. B. Making chemicals with electricity. *Science* **364**, 734–735 (2019).
22. Wismann, S. T. et al. Electrified methane reforming: a compact approach to greener industrial hydrogen production. *Science* **364**, 756–759 (2019).
23. Bai, Z., Chen, H., Li, B. & Li, W. Catalytic decomposition of methane over activated carbon. *J. Anal. Appl. Pyrolysis* **73**, 335–341 (2005).
24. Gao, Z., Kobayashi, M., Wang, H., Onoe, K. & Yamaguchi, T. Methane conversion in thermal diffusion column reactor with carbon rod as pyrogen. *Fuel Process. Technol.* **88**, 996–1001 (2007).
25. Shields, B. J. et al. Bayesian reaction optimization as a tool for chemical synthesis. *Nature* **590**, 89–96 (2021).
26. Wang, Y., Chen, T.-Y. & Vlachos, D. NEXTorch: a design and Bayesian optimization toolkit for chemical sciences and engineering. *J. Chem. Inf. Model.* **61**, 5312–5319 (2021).
27. Frenklach, M. Reaction mechanism of soot formation in flames. *Phys. Chem. Chem. Phys.* **4**, 2028–2037 (2002).
28. Yablonsky, G. S., Constales, D. & Marin, G. B. Equilibrium relationships for non-equilibrium chemical dependencies. *Chem. Eng. Sci.* **66**, 111–114 (2011).
29. Silva, G. D. Mystery of 1-vinylpropargyl formation from acetylene addition to the propargyl radical: an open-and-shut case. *J. Phys. Chem. A* **121**, 2086–2095 (2017).
30. Mansurov, Z. A. Soot formation in combustion processes. *Combust. Explos. Shock Waves* **41**, 727–744 (2005).
31. Saadatjou, N., Jafari, A. & Sahebdelfar, S. Ruthenium nanocatalysts for ammonia synthesis: a review. *Chem. Eng. Commun.* **202**, 420–448 (2015).
32. Qin, R. et al. Alkali ions secure hydrides for catalytic hydrogenation. *Nat. Catal.* **3**, 703–709 (2020).
33. Dahl, S., Sehested, J., Jacobsen, C. J. H., Törnqvist, E. & Chorkendorff, I. Surface science based microkinetic analysis of ammonia synthesis over ruthenium catalysts. *J. Catal.* **192**, 391–399 (2000).
34. Bowker, M., Parker, I. B. & Waugh, K. C. Extrapolation of the kinetics of model ammonia synthesis catalysts to industrially relevant temperatures and pressures. *Appl. Catal.* **14**, 101–118 (1985).
35. Wu, L., Hu, S., Yu, W., Shen, S. & Li, T. Stabilizing mechanism of single-atom catalysts on a defective carbon surface. *NPJ Comput. Mater.* **6**, 1–8 (2020).
36. Özçelik, V. O., Gurel, H. H. & Ciraci, S. Self-healing of vacancy defects in single-layer graphene and silicene. *Phys. Rev. B* **88**, 045440 (2013).
37. Ye, T.-N. et al. Vacancy-enabled N_2 activation for ammonia synthesis on an Ni-loaded catalyst. *Nature* **583**, 391–395 (2020).
38. Gong, Y. et al. Ternary intermetallic LaCoSi as a catalyst for N_2 activation. *Nat. Catal.* **1**, 178–185 (2018).
39. Kitano, M. et al. Ammonia synthesis using a stable electride as an electron donor and reversible hydrogen store. *Nat. Chem.* **4**, 934–940 (2012).
40. Shi, M.-M. et al. Au sub-nanoclusters on TiO_2 toward highly efficient and selective electrocatalyst for N_2 conversion to NH_3 at ambient conditions. *Adv. Mater.* **29**, 1606550 (2017).

Data availability

The data that support the findings of this study are available within this article and its Supplementary Information. Further data are available from the corresponding authors on reasonable request. Source data are provided with this paper.

Code availability

The code used for active learning has been deposited in the Code Ocean repository (ref. [41]).

41. Dong, Q. et al. Active learning for programmable heating and quenching. Code Ocean https://doi.org/10.24433/CO.1790371.v1 (2021).

Acknowledgements We acknowledge the support from the University of Maryland A. James Clark School of Engineering. We acknowledge the Maryland NanoCenter, the Surface Analysis Center and the AIM Lab. We thank M. R. Zachariah and D. J. Kline from the University of California, Riverside for their help on the temperature measurements. We thank E. Schulman from the University of Maryland, College Park for her help on the energy cost calculations. D.L. acknowledges the support from the Department of Energy, Office of Fossil Energy (DE-FE0031877). D.G.V. acknowledges the support from the Department of Energy, Office of Energy Efficiency and Renewable Energy and Advanced Manufacturing Office (DE-EE0007888-9.5). The Delaware Energy Institute acknowledges the support and partnership of the State of Delaware in furthering the essential scientific research being conducted through the RAPID projects. Y.J. acknowledges the support from the National Science Foundation (NSF EFRI DCheM-2029425).

Author contributions L.H., Q.D. and Y.Y. came up with the design concept. Q.D. and S.C. designed the reactor and collected the data for CH_4 pyrolysis. Q.D., Y.Y. and J.G. collected the data for NH_3 synthesis. K.A., H.E.T. and D.G.V. carried out the simulation for CH_4 pyrolysis and the energy cost calculation. S.S. and Y.W. conducted the active learning. Q.D. and X.W. performed the temperature measurements. Y.P., C.Z. and B.Y. carried out the modelling for the temperature profile of the gas molecules. J.G. collected the digital images. Q.D. and Y.Y. conducted the spectroscopic and microscopic analysis. K.A., D.G.V., H.Z. and Y.J. carried out the simulation for NH_3 synthesis. I.G.K. helped analyse the overall results. L.H., Q.D., Y.Y. and A.H.B. collectively wrote the paper, together with input from all authors. L.H., D.L. and D.G.V. supervised the project. All authors discussed the results and contributed to the final manuscript.

Competing interests L.H., Y.Y., Q.D. and D.L. report a patent application of 'High-temperature shock heating for thermochemical reactions' filed on 12 March 2021, US application no. PCT/US2021/022204.

Additional information

Supplementary information The online version contains supplementary material available at https://doi.org/10.1038/s41586-022-04568-6.

Correspondence and requests for materials should be addressed to Dionisios G. Vlachos, Dongxia Liu or Liangbing Hu.

Peer review information *Nature* thanks the anonymous reviewers for their contribution to the peer review of this work.